



Original article

Synthesis and biological evaluation of novel bifendate derivatives bearing 6, 7-dihydro-dibenzo[*c,e*]azepine scaffold as potent P-glycoprotein inhibitors

Xiaoke Gu^{a,b,1}, Zhiguang Ren^{c,1}, Xiaobo Tang^{a,b}, Hui Peng^{c,**}, Qing Zhao^c, Yisheng Lai^{a,b}, Sixun Peng^{a,b}, Yihua Zhang^{a,b,*}

^a State Key Laboratory of Natural Medicines, China Pharmaceutical University, Nanjing 210009, People's Republic of China

^b Center of Drug Discovery, China Pharmaceutical University, Nanjing 210009, People's Republic of China

^c Department of Molecular Immunology, Institute of Basic Medical Sciences, Beijing 100850, People's Republic of China

ARTICLE INFO

Article history:

Received 7 December 2011

Received in revised form

11 February 2012

Accepted 16 February 2012

Available online 25 February 2012

Keywords:

Bifendate

dibenzo[*c,e*]azepine

P-gp inhibitor

Multidrug resistance

ABSTRACT

Overexpression of P-glycoprotein (P-gp) is one of the major problems in successful treatment of cancers. To find new P-gp inhibitors, a series of bifendate (DDB) derivatives bearing dibenzo[*c,e*]azepine scaffold were synthesized and evaluated. Compound **4i** more potently reversed P-gp-mediated multidrug resistance (MDR) than DDB and verapamil (VRP) by blocking P-gp mediated drug efflux function and increasing drug accumulation in K562/A02 MDR cells, and persisted longer chemo-sensitizing effect (>24 h) than VRP (<6 h). Interestingly, unlike VRP, **4i** showed no stimulation on the P-gp ATPase activity, suggesting it is not a substrate of P-gp. Given the low intrinsic cytotoxicity of **4i** *in vitro*, it may represent a promising lead for developing therapeutics targeting P-gp-mediated MDR in combinational cancer chemotherapy.

© 2012 Elsevier Masson SAS. All rights reserved.

1. Introduction

The emergence of multidrug resistance (MDR) is regarded as the major barrier to successful chemotherapy in cancer patients [1]. A primary mechanism of MDR involves the overexpression of P-gp, a member of ATP-binding cassette (ABC) transporter superfamily, in the plasma membrane of drug-resistant cells [2]. P-gp mainly utilizes energy derived from ATP hydrolysis to actively export anticancer drugs out of tumor cells, leading to the reduction of intracellular drug levels and consequent drug insensitivity. Direct inhibition of P-gp with specific inhibitors is considered as a suitable and attractive approach to overcome P-gp-mediated MDR [3], and considerable attempts have been made to develop P-gp inhibitors during past decades. However, until now, no drug of this class has been approved for many reasons, such as low selectivity, poor potency, inherent toxicity and/or adverse pharmacokinetic

interaction with anticancer drugs. Therefore, there is a clear and urgent requirement for developing novel effective P-gp inhibitors [4].

Nowadays, the strategies for generating such compounds have been extended to the natural food, herbal extracts and their synthetic derivatives [5], which are reported to be inhibitors of one or more ABC drug efflux pumps, and usually are low in toxicity and well tolerated in the human body [6,7]. Recently, it has been demonstrated that lignans extracted from *Schisandra chinensis* Baill (Wuweizi) and its components deoxyschizandrin and schisandrol A have the ability to restore drug sensitivity at non-toxic concentrations via direct interaction with P-gp [8,9]. Some other synthetic schisanderin derivatives exhibit the similar effects as the natural products. Bifendate (DDB) is an analog of schizandrin C [10], and has been widely used for the treatment of chronic viral hepatitis B with few side effects for more than 20 years in China. Interestingly, recent investigations demonstrated that DDB had MDR reversal activity *in vitro* and *in vivo* by increasing intracellular accumulation of anticancer drugs and promoting cancer cell apoptosis through inhibiting P-gp [11]. More importantly, DDB shows no pharmacokinetic interactions with anticancer drugs [11]. However, DDB requires high doses to reverse MDR, and the potency is lower as compared with the classical P-gp inhibitor, verapamil (VRP). Therefore, development

* Corresponding author. State Key Laboratory of Natural Medicines, China Pharmaceutical University, Nanjing 210009, People's Republic of China. Tel./fax: +86 25 83271015.

** Corresponding author. Tel.: +86 10 66932339; fax: +86 10 68159436.

E-mail addresses: p_h2002@hotmail.com (H. Peng), zyhtgd@163.com (Y. Zhang).

¹ These two authors contributed equally to this work.

of novel DDB derivatives with high chemo-sensitizing effects is of great importance.

To date, target-based drug design methods, such as virtual screening or de novo design, are not suited for identification of new P-gp inhibitors due to the low resolution of available crystal structure (only 3.8 Å) and the multispecific interaction patterns of P-gp [12]. Our design strategy was based on structures-activity relationship (SAR) studies of P-gp inhibitors as previously summarized in literatures [3,5,13–16]. In brief, potent P-gp inhibitors were characterized with two or three aromatic moieties, a tertiary nitrogen atom, one to three hydrogen-bond acceptors, and/or one hydrogen-bond donor. Keeping these in mind, and in view of the crucial role of sixalkoxyl biphenyl moiety in DDB for pharmacological activity [17], various N-substituted tertiary amines were respectively combined to the sixalkoxyl biphenyl structure forming compounds (**4a–j**) each with a 6,7-dihydro-dibenzo[*c,e*]azepine ring to improve the P-gp inhibitory effect and affinity of DDB with P-gp. And some of the compounds (**4a–d**) were further oxidized to the corresponding amides (**5a–d**) to examine the influence of amidation-modification of the tertiary amine on P-gp inhibitory activity. Thus, fourteen target compounds were designed and synthesized, and their ability to interact with P-gp transporter in K562/A02 cells which overexpress P-gp was subsequently evaluated.

2. Chemistry

The synthetic routes of the target compounds **4a–j** and **5a–d** are depicted in Scheme 1. The starting material DDB was treated with excess LiAlH₄ in THF to give the corresponding diol **2**, which was then converted to the methylsulfonic acid ester **3** by methylsulfonfyl chloride. The nucleophilic substitution of **3** by various amines afforded the desired products 6,7-dihydro-dibenzo[*c,e*]azepine (**4a–j**). Further oxidation of **4a–d** with KMnO₄ provided the corresponding amides **5a–d**, respectively.

3. Results and discussion

3.1. Biological evaluation

3.1.1. Cytotoxicity assays

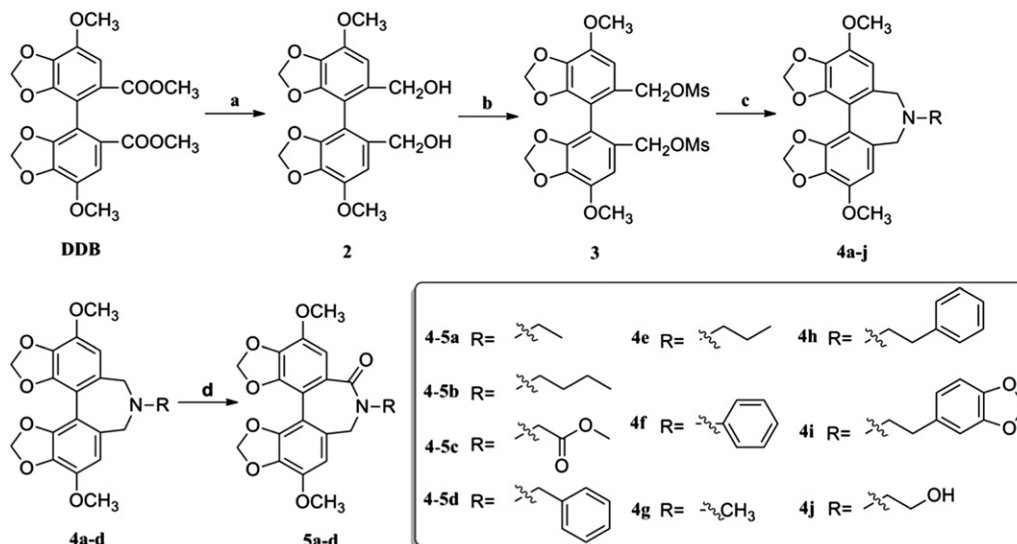
The cytotoxicities of the target compounds against K562 and its drug-resistant subline K562/A02 cells which overexpress P-gp were

determined by MTS assay. A well-known anticancer drug Adriamycin (ADR) was used as the positive control. As shown in Table 1, the target compounds displayed low intrinsic cytotoxicity since their IC₅₀ values were at a high micromolar level. As expected, K562/A02 cells were significantly resistant to ADR: the IC₅₀ value (46.69 μM) is 108-fold higher than that of parental non-resistant cells. Interestingly, both K562 and K562/A02 cells were almost equally insensitive to the target compounds, indicating that, unlike ADR, they were not likely to be substrates of P-gp. Based on the IC₅₀s determined above, compounds at concentrations below IC₁₀ were used in the following MDR reversal experiments.

3.1.2. Effect of the target compounds on Rh123 and ADR accumulation

The effect of the target compounds (10 μM, IC₁₀) on the intracellular accumulation of Rhodamine 123 (Rh123), a fluorescent substrate of P-gp) in K562/A02 cells was assayed by flow cytometry. The classical P-gp inhibitor verapamil (VRP) was used as a positive control. As shown in Fig. 1 A, treatment with VRP led to a significant increase of intracellular Rh123 level in K562/A02 cells, the accumulation fold change was 8.5 larger than that of vehicle control (0.1% DMSO). Rh123 accumulation in the cells treated with 10 μM DDB showed a slight increase and the accumulation fold change was only 1.2, indicating that DDB had weak P-gp inhibitory effect, which is consistent with previous report [11]. Interestingly, this effect was enhanced greatly by the chemical modifications of DDB. As observed in Fig. 1 A, the Rh123 accumulation fold change of most target compounds was significantly higher than that of DDB. Compounds **4h** and **4i** obviously increased the intracellular Rh123 level in K562/A02 cells, and their accumulation fold change was 10.1 and 11.2, respectively, which was higher than that of VRP. Compound **4d** exhibited the same effect on Rh123 accumulation as VRP.

In order to further investigate the effect of **4d**, **4h** and **4i** on P-gp, their dose-response effects on Rh123 accumulation in K562/A02 and parental sensitive K562 cells were respectively determined by flow cytometry. As shown in Fig. 1 B, VRP, **4d**, **4h** and **4i** produced a significant increase in Rh123 accumulation in K562/A02 cells in a dose-dependent manner, but not in P-gp-negative K562 cells, suggesting that the effect of these compounds on Rh123 accumulation is likely via inhibiting P-gp. Furthermore, ADR, another substrate of P-gp, was used to test the inhibitory effect of **4i** on P-gp



Scheme 1. Synthesis of the target compounds. Reagents and conditions: a) LiAlH₄, THF, 0 °C-rt, 4 h; b) methylsulfonfyl chloride, Et₃N, CH₂Cl₂, rt, 6 h; c) acetonitrile, Et₃N, 40 °C, 6–8 h; d) KMnO₄, hexadecyl trimethyl ammonium bromide, CH₂Cl₂, reflux, 0.5–1 h.

Table 1
IC₅₀ values of target compounds against K562 and K562/A02 cells.

Compound	IC ₅₀ (μM) ^a		Compound	IC ₅₀ (μM) ^a	
	K562/A02	K562		K562/A02	K562
4a	117.2	125	4i	46.88	53.72
4b	>100	77.47	4j	>200	>200
4c	>100	>100	5a	>100	>100
4d	111.9	>200	5b	44.6	41.71
4e	87.64	106	5c	>100	>100
4f	>100	>100	5d	53.37	43.48
4g	107	140.3	ADR	46.69	0.43
4h	34.11	45.36			

^a IC₅₀ values are expressed as means of triplicate experiments.

using the similar assay above. As shown in Fig. 1 C, **4i** and VRP increased the intracellular ADR level in K562/A02 cells in a dose-dependent manner, but such effect was not observed in K562 cells. Collectively, both Rh123 and ADR accumulation fold changes of **4i** were obviously greater than that of DDB and VRP, suggesting that **4i** may be a potent P-gp inhibitor.

3.1.3. Inhibitory effect of **4i** on P-gp-mediated Rh123 efflux function

To investigate if **4i** can reverse P-gp-mediated drug efflux function, intracellular Rh123 was photographed under a fluorescence microscope (Fig. 2 A–C) and determined using flow cytometry (Fig. 2 D). As expected, the parental sensitive K562 cells retained most of the fluorescence dye (Fig. 2 A1), while K562/A02 cells which overexpress P-gp effluxed the dye efficiently and there was no fluorescence in the cells after 60-min incubation (Fig. 2 A2). Interestingly, **4i** significantly blocked the efflux in a dose-dependent manner, resulting in significant retention of Rh123 in K562/A02 cells (Fig. 2 B1–3), and displayed much higher potency than VRP at the same doses (Fig. 2 C1–3). As shown in Fig. 2 D, intracellular Rh123 level in K562/A02 cells treated with 2.5 μM **4i** was almost the same as K562 cells, indicating **4i** completely inhibited P-gp efflux function (Fig. 2 D1). VRP, however, even up to 5 μM, could not achieve the similar effect as **4i** (Fig. 2 D2). These results supported the argument that **4i** displayed stronger inhibitory effect on P-gp-mediated drug efflux function than the classical P-gp inhibitor VRP.

3.1.4. Chemo-sensitizing effect of target compounds

To confirm the reversal effect of novel DDB derivatives on P-gp mediated MDR, the cytotoxicity of ADR against K562/A02 cells and K562 cells was evaluated in the presence or absence of the DDB derivatives at various concentrations (ch: 5 μM, cm: 2.5 μM and cl: 1.25 μM) by MTS assay, using VRP as the positive control. As shown in Fig. 3, the target compounds and VRP (ch, red bar) had little inhibitory effect on the survival of K562/A02 and K562 cells at

5.0 μM (high dose in this experiment), each only producing ~10% cell killing. Anticancer drug ADR, a well-known P-gp substrate, was also non-toxic to K562/A02 and K562 cells at 3.5 μM and 0.05 μM, respectively (Fig. 3, green bar). However, its cytotoxicity against K562/A02 cells was increased to various extents in the combination with target compounds or VRP (Fig. 3 A). Noteworthy, **4h** and **4i** significantly enhanced the sensitivity of K562/A02 cells to ADR at 2.5 μM concentration. The most active compound **4i** showed potent chemo-sensitizing effect even at 1.25 μM, because the survival rate of K562/A02 cells treated with **4i** or ADR alone was 98% and 95%, respectively, while the survival rate of the cells treated by combination of **4i** and ADR was dramatically reduced to 30%. Furthermore, the survival rate of K562/A02 cells was decreased to 8% and 6% by combinational treatment of 2.5 μM or 5 μM **4i** with ADR, respectively (Fig. 3 A). On the other hand, VRP displayed much poorer chemo-sensitizing effect compared with **4i** under the same conditions. Even if K562/A02 cells were treated with 5 μM VRP, the survival rate was still higher than 50%. These results indicated that the DDB derivatives, especially **4i**, significantly potentiated the cytotoxicity of ADR in K562/A02 cells in a dose-dependent manner. Moreover, no such chemo-sensitizing effect was observed in P-gp-negative K562 cells (Fig. 3 B), suggesting that the DDB derivatives exert chemo-sensitizing effect via inhibition of P-gp function.

3.1.5. Effect of target compounds on the expression of mRNA and protein levels of P-gp

It is known that P-gp-mediated MDR can be reversed either by inhibiting transport function of P-gp or decreasing its expression level [18]. Since we have already demonstrated the DDB derivatives exert chemo-sensitizing effect via inhibition of P-gp function, we next determined whether the active compounds **4d**, **4h** and **4i** exhibited an inhibitory effect on the expression of P-gp at mRNA and protein levels, using RT-PCR and Western blot, respectively. As shown in Fig. 4, no marked difference in P-gp expression at mRNA (Fig. 4 A) or protein level (Fig. 4 B) was observed in K562/A02 cells treated with target compounds (5 μM) for 72 h compared to vehicle (0.1% DMSO). These results suggest that the DDB derivatives exert the MDR reversal activity by inhibiting P-gp drug efflux function and not by decreasing P-gp expression.

3.1.6. Duration of chemo-sensitizing effect of **4i** toward ADR in K562/A02 cells

Next, the duration of chemo-sensitizing effect of DDB derivative **4i** was determined. Briefly, K562/A02 cells were incubated with **4i** (2.5 μM) or VRP (10 μM) for 24 h, and then each compound in the culture media was washed out, leaving cells with fresh media. ADR at various concentrations was then added to the culture at 0, 6, 12, or 24 h after the removal of the compounds to examine the duration of the MDR-reversal activity of **4i** or VRP. In the absence of **4i** or

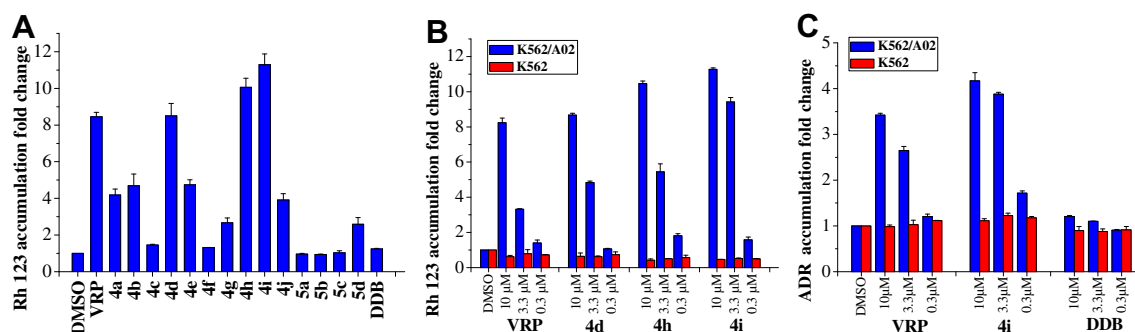


Fig. 1. The effect of the target compounds on the intracellular accumulation of Rh123 (0.5 μM) or ADR (0.5 μM). The relative values were identified by dividing the fluorescence intensity of each measurement treated with compound or VRP by that of incubation with 0.1% DMSO. Data represents means ± S.D. of three independent experiments.

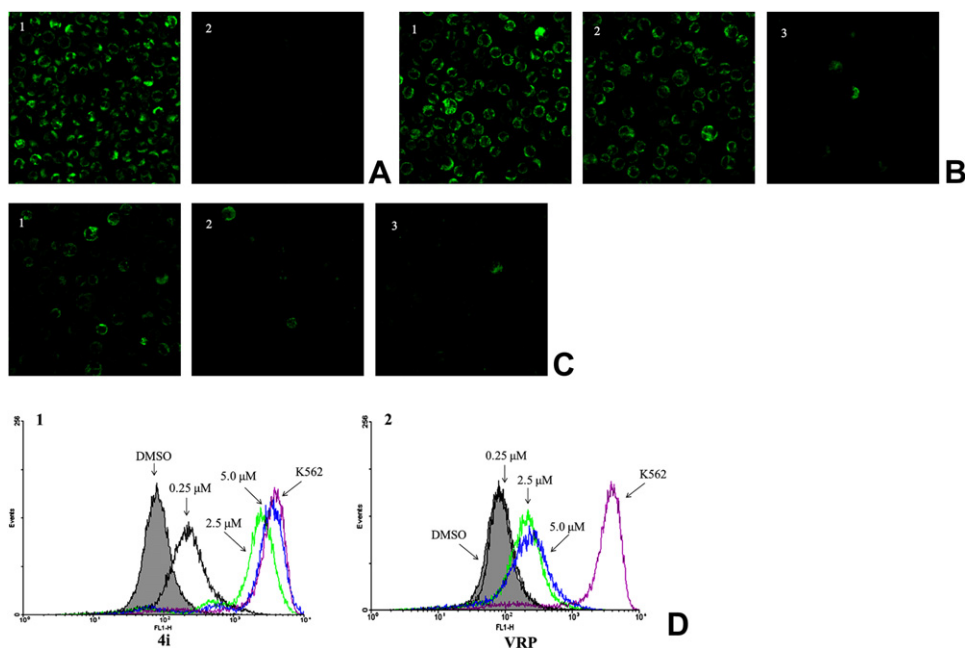


Fig. 2. Inhibitory effect of **4i** on P-gp efflux function. (A) Intracellular Rh123 in K562 (A1) or K562/A02 (A2) cells was photographed under a fluorescence microscope. (B–C) Intracellular Rh123 in K562/A02 cells treated with various concentrations of **4i** (B1: 5.0 μ M, B2: 2.5 μ M, B3: 0.25 μ M) compared with VRP (C1: 5.0 μ M, C2: 2.5 μ M, C3: 0.25 μ M). (D) Dose response of **4i** or VRP in retaining Rh123 accumulation in K562/A02 cells. The purple line represents the level of Rh123 accumulation in K562 cells, serving as a control. (For interpretation of the references to colour in this figure legend, the reader is referred to the web version of this article.)

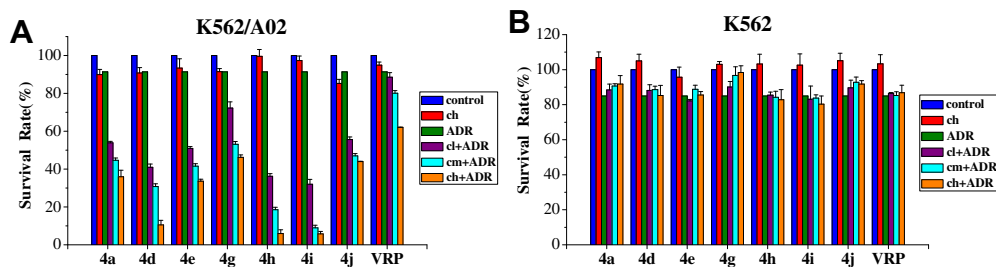


Fig. 3. Chemo-sensitizing effect of the target compounds. The cytotoxicity of ADR against K562/A02 cells and K562 cells in the presence or absence of the target compounds at various concentrations (cl: 1.25 μ M; cm: 2.5 μ M; ch: 5.0 μ M) was evaluated by MTS assay. The classical P-gp inhibitor VRP was used as a positive control. Survival rate was expressed as percentage mean of cell growth \pm S.D. with respect to the control without any treatment of three independent experiments. (For interpretation of the references to colour in this figure legend, the reader is referred to the web version of this article.)

VRP, the IC_{50} s were 33.59, 35.15, 54.11, and 51.67 μ M when ADR was added at 0, 6, 12, or 24 h to the culture, respectively (Fig. 5). As observed previously, both **4i** and VRP significantly sensitized K562/A02 cells to ADR right after they were removed, the IC_{50} s of ADR were 1.78 and 12.92 μ M, respectively (Fig. 5 A). And IC_{50} s of ADR were 26.06, 51.05 and 51.40 μ M when ADR was added at 6, 12 and 24 h after the removal of VRP, respectively. The IC_{50} s were almost equal to those obtained in the control group which was not exposed to any compounds. In sharp contrast, **4i** showed significant reversal activity even at 24 h after exposure (Fig. 5 D). The IC_{50} s of ADR were 2.47, 5.03, and 10.29 μ M when ADR was added to the cells at 6, 12, and 24 h after removal of **4i**. Hence, one conclusion can be drawn from these results: **4i** exhibited potent chemo-sensitizing effect, which persisted for much longer time (>24 h) compared with positive control VRP (<6 h) after removal of the agent from the culture.

3.1.7. Effect of **4i** on P-gp ATPase activity

Since efflux of drug by P-gp normally requires energy from ATP hydrolysis by the ATPase, which is generally stimulated in the presence of P-gp substrate. Among the identified reversal agents,

some compounds (e.g., VRP) also stimulate the basal ATPase activity, thus behaving like a substrate or competitive inhibitor for the pumps [3]. Therefore, the MDR-reversal effect is exerted only at a higher concentration which might easily reach toxic ranges,

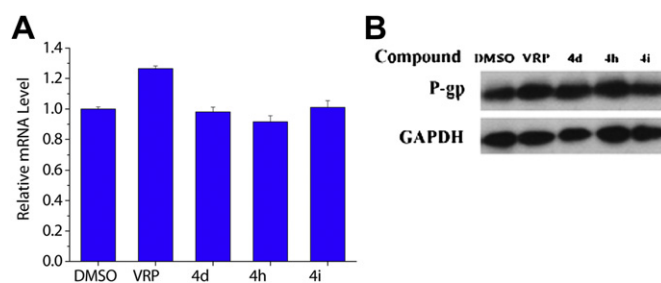


Fig. 4. Effects of active compounds on P-gp mRNA and protein expression level. (A) The relative P-gp mRNA level treated with compounds was expressed as fold change of the control cultures (in the presence of 0.1% DMSO). Data shown are mean \pm S.D. from three independent experiments. (B) Effect of target compounds on the expression of P-gp at protein level. Independent experiments were performed at least three times, and a representative experiment is shown.

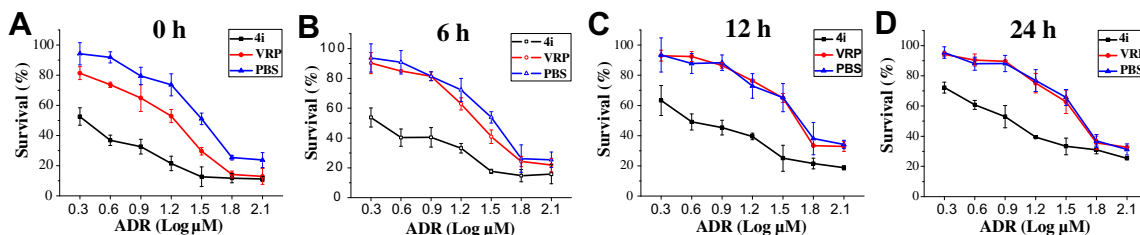


Fig. 5. Duration of chemo-sensitizing effect of **4i** and VRP toward ADR in K562/A02 cells after incubation and subsequent washout. Cell proliferation was determined by MTS assay. Data represents means \pm SE of triplicate determinations.

leading to a serious side effect [19]. To learn whether **4i** is a substrate of P-gp, its effect on P-gp ATPase activity was determined according to a previously described method [20]. In brief, the activity of P-gp ATPase was measured in the presence or absence of Na_3VO_4 (as a negative control), **4i**, or VRP (as a positive control). Thus, the luminescence was detected in a luminometer, and the luminescence value of each sample represented its ATP level, which is negatively correlated with the activity of P-gp ATPase. As shown in Table 2, VRP caused a significant increase in the activity of P-gp ATPase ($P < 0.01$) compared with the untreated group, while **4i** or Na_3VO_4 showed no stimulation of the P-gp ATPase activity, indicating that **4i** was not a substrate of P-gp.

3.2. Structure-activity relationships

Based on the results above, structure-activity relationships (SARs) of DDB derivatives could be drawn as follows: compounds with the dibenzo[*c,e*]azepine scaffold more strongly reversed P-gp-mediated MDR than DDB and VRP. The substitutes at nitrogen atom in dibenzo[*c,e*]azepine significantly affected the intensity of P-gp inhibitory effect. Compounds bearing a third benzene ring except **4f** showed more potent inhibitory effect on the drug efflux function of P-gp than those bearing an alkyl group (**4d**, **4h** and **4i** vs. **4a**, **4b**, **4e** and **4g**). Introducing an electron donating substitute to the third benzene ring, such as methylenedioxy group, could increase the intensity of P-gp inhibitory effect (**4i** vs. **4h**). In addition, the length of the carbon chain linked to the third benzene ring and nitrogen atom also played a crucial role in inhibition of P-gp. The compounds with a two-carbon chain showed higher inhibitory effect on P-gp than the compounds with a zero- or one-carbon chain (**4h** vs. **4d**, **4f**). Interestingly, when dibenzo[*c,e*]azepine was oxidized to dibenzo[*c,e*]azepine-5-one, the P-gp inhibitory activity was significantly reduced (**5a–d** vs. **4a–d**). One plausible explanation is that conversion of amine to amide might reduce the electron density of nitrogen atom, leading to low affinity with P-gp and consequent poor P-gp inhibitory effect. All these trends above are highly consistent with SAR analyses previously reported [3,5,13–16], and hence verify our previous presumption that the various N-substituted tertiary amines play a significant role in the MDR reversal activity of these novel DDB derivatives. However, the

Table 2
Effect of **4i** on P-gp ATPase activity.

Compound	Concentration (μM)	Luminescence (relative light units) ^a
Untreated	0	242,328 \pm 1398
VRP	200	231,282 \pm 293*
Na_3VO_4	200	281,688 \pm 439*
4i	40	283,026 \pm 715*

* $P < 0.01$ vs. untreated group, determined by Student's *t* test.

^a Relative light units represent the level of ATP in the sample, exhibiting a negative relationship with activity of P-gp ATPase. Data are expressed as means \pm SDs of three separate experiments.

precise SARs remain further investigation when more DDB derivatives bearing a dibenzo[*c,e*]azepine moiety will be available in the near future.

4. Conclusions

In summary, a series of novel DDB derivatives containing dibenzo[*c,e*]azepine scaffold were synthesized and their inhibitory effect on P-gp was evaluated using the classical P-gp inhibitor VRP as a positive control. Most of the target compounds showed potent chemo-sensitizing effect on K562/A02 cells, and compounds **4h** and **4i** more potently blocked the drug efflux function of P-gp and increased the accumulation of drug in K562/A02 cells than VRP but did not inhibit expression of P-gp at mRNA and protein level. Additionally, the chemo-sensitizing effect of **4i** persisted much longer (>24 h) than VRP (<6 h). Interestingly, unlike VRP, **4i** did not stimulate the activity of P-gp ATPase, suggesting it is not a substrate of P-gp. Given the low intrinsic cytotoxicity of **4i** *in vitro*, it might represent a promising lead for developing therapeutics targeting P-gp-mediated MDR in combinational cancer chemotherapy. Further intensive investigations are still in progress.

5. Experimental protocols

5.1. Chemical analysis

Melting points were determined on a Mel-TEMP II melting point apparatus and uncorrected.

All of the synthesized compounds were purified by column chromatography (CC) on silica gel 60 (200–300 mesh) or thin layer chromatography (TLC) on silica gel 60 F254 plates (250 mm; Qingdao Ocean Chemical Company, China). Subsequently, they were routinely analyzed by IR (Shimadzu FTIR-8400S), ^1H NMR and ^{13}C NMR (Bruker ACF-300Q, 300 MHz), and MS (Hewlett–Packard 1100 LC/MSD spectrometer). High resolution mass spectra (HRMS) were recorded on Agilent technologies LC/MSD TOF. All solvents were reagent grade and, when necessary, were purified and dried by standards methods. Solutions after reactions and extractions were concentrated using a rotary evaporator operating at a reduced pressure of ca. 20 Torr. Organic solutions were dried over anhydrous sodium sulfate.

5.2. Synthesis of 4,4'-dimethoxy-5,6,5',6'-dimethylenedioxy-2,2'-dibenzyl dimethanol **2**

To a solution of DDB (4 g, 9.56 mmol) in dry THF (50 mL) at 0°C was added LiAlH_4 (1.09 g, 28.68 mmol) portionwise. The mixture was stirred for 4 h at room temperature, cooled to 0°C , distilled water was added slowly along the flask wall to the mixture until no hydrogen generated. The mixture was filtered and washed with CH_2Cl_2 several times. The filtrate was diluted with water and extracted with CH_2Cl_2 . The organic layer was washed with brine,

dried with anhydrous sodium sulfate, filtered and evaporated in vacuum to give the title compound as a white solid (2.9 g), yield: 85%; mp: 170–171 °C (lit. [21], 172–173 °C). ESI-MS: m/z 385 $[M + Na]^+$.

5.3. Synthesis of 4,4'-dimethoxy-5,6,5',6'-dimethylenedioxy-2,2'-dibenzyl dimethanesulfonate **3**

To a stirred solution of compound **2** (2 g, 5.5 mmol) in CH_2Cl_2 20 mL, triethylamine (2.33 ml, 16.5 mmol) was added followed by the drop wise addition of methanesulfonyl chloride (1.28 ml, 16.5 mmol). The reaction mixture was stirred for 6 h at room temperature. The progress of reaction was monitored by TLC. After the completion of reaction, the reaction mixture was diluted with water, extracted with CH_2Cl_2 and the organic layer was washed with brine, dried with anhydrous sodium sulfate, filtered. Removal of the solvent in vacuo gave the mesylated alcohol **3**, which was used as such in the next step.

5.4. General procedure for the preparation of **4a–j**

A solution of **3** (0.19 mmol), triethylamine (0.38 mmol) and substituted amine (0.76 mmol) in acetonitrile (15 ml) was stirred at 40 °C for 6–8 h, the reaction mixture was diluted with saturated aqueous $NaHCO_3$ and extracted with EtOAc. The organic layer was washed with brine, dried with anhydrous sodium sulfate, filtered and evaporated in vacuum. The crude product was purified by column chromatography ($CH_2Cl_2/EtOAc = 10:1–5:1$) to yield the title compound, respectively.

5.4.1. 6-Ethyl-3,9-dimethoxy-1,2-methylenedioxy-10,11-methylenedioxy-6,7-dihydro-5H-dibenz[c,e]azepine (**4a**)

The title compound was obtained starting from **3** and ethylamine hydrochloride. As a white solid, yield: 87%; mp: 151–153 °C. Analytical data for **4a**: 1H NMR ($CDCl_3$, 300 MHz, δ ppm): 1.06 (t, 3H, CH_3 , $J = 7.2$ Hz), 2.67–2.85 (m, 2H, NCH_2), 3.33 (d, 2H, NCH_2 , $J = 12.6$ Hz), 3.73 (d, 2H, NCH_2 , $J = 12.6$ Hz), 3.96 (s, 6H, $2 \times OCH_3$), 6.01 (s, 2H, OCH_2O), 6.10 (s, 2H, OCH_2O), 6.64 (s, 2H, $2 \times Ar-H$); ^{13}C NMR ($CDCl_3$, 75 MHz, δ ppm): δ 12.7, 48.8, 54.2, 56.8, 101.8, 109.6, 110.5, 129.2, 134.9, 142.9, 145.8; IR (KBr, cm^{-1}): ν 3447, 1635, 1437, 1381, 1308, 1142, 1101, 1045, 759, 641; ESI-MS: m/z 372 $[M + H]^+$; HRMS (ESI m/z) for $C_{20}H_{22}NO_6$ calcd 372.1447, found 372.1452 $[M + H]^+$.

5.4.2. 6-Butyl-3,9-dimethoxy-1,2-methylenedioxy-10,11-methylenedioxy-6,7-dihydro-5H-dibenz[c,e]azepine (**4b**)

The title compound was obtained starting from **3** and butylamine. As a white solid, yield: 86%; mp: 144–146 °C. Analytical data for **4b**: 1H NMR ($CDCl_3$, 300 MHz, δ ppm): 0.96 (t, 3H, CH_3 , $J = 7.2$ Hz), 1.32–1.45 (m, 2H, CH_2), 1.53–1.59 (m, 2H, CH_2), 2.38–2.60 (m, 2H, NCH_2), 3.18 (d, 2H, NCH_2 , $J = 12.5$ Hz), 3.53 (d, 2H, NCH_2 , $J = 12.5$ Hz), 3.95 (s, 6H, $2 \times OCH_3$), 5.99 (s, 2H, OCH_2O), 6.09 (s, 2H, OCH_2O), 6.56 (s, 2H, $2 \times Ar-H$); ^{13}C NMR ($CDCl_3$, 75 MHz, δ ppm): δ 14.1, 20.8, 30.1, 55.1, 56.7, 101.7, 109.2, 110.7, 129.2, 134.8, 142.8, 145.7; IR (KBr, cm^{-1}): ν 3446, 3020, 2944, 2867, 2778, 1641, 1490, 1463, 1435, 1384, 1304, 1138, 1163, 1102, 1048, 756, 697; ESI-MS: m/z 400 $[M + H]^+$; HRMS (ESI m/z) for $C_{22}H_{26}NO_6$ calcd 400.1760, found 400.1765 $[M + H]^+$.

5.4.3. 6-(Methoxycarbonyl)methyl-3,9-dimethoxy-1,2-methylenedioxy-10,11-methylenedioxy-6,7-dihydro-5H-dibenz[c,e]azepine (**4c**)

The title compound was obtained starting from **3** and glycine methyl ester hydrochloride. As a white solid, yield: 77%; mp: 156–158 °C. Analytical data for **4c**: 1H NMR ($CDCl_3$, 300 MHz,

δ ppm): 3.25 (d, 1H, NCH_2 , $J = 16.2$ Hz), 3.30 (d, 2H, NCH_2 , $J = 12.6$ Hz), 3.45 (d, 1H, NCH_2 , $J = 16.2$ Hz), 3.57 (d, 2H, NCH_2 , $J = 12.6$ Hz), 3.79 (s, 3H, OCH_3), 3.94 (s, 6H, $2 \times OCH_3$), 5.96 (s, 2H, OCH_2O), 6.10 (s, 2H, OCH_2O), 6.58 (s, 2H, $2 \times Ar-H$); ^{13}C NMR ($CDCl_3$, 75 MHz, δ ppm): δ 52.0, 55.4, 56.7, 101.7, 109.3, 110.6, 128.6, 135.0, 142.9, 145.8, 171.1; IR (KBr, cm^{-1}): ν 3447, 2943, 2366, 1739, 1640, 1435, 1384, 1307, 1169, 1142, 1100, 1042, 783, 668; ESI-MS: m/z 416 $[M + H]^+$; HRMS (ESI m/z) for $C_{21}H_{22}NO_8$ calcd 416.1345, found 416.1350 $[M + H]^+$.

5.4.4. 6-Benzyl-3,9-dimethoxy-1,2-methylenedioxy-10,11-methylenedioxy-6,7-dihydro-5H-dibenz[c,e]azepine (**4d**)

The title compound was obtained starting from **3** and benzylamine. As a white solid, yield: 81%; mp: 178–179 °C. Analytical data for **4d**: 1H NMR ($CDCl_3$, 300 MHz, δ ppm): 3.21 (d, 2H, NCH_2 , $J = 12.5$ Hz), 3.47 (d, 2H, NCH_2 , $J = 12.5$ Hz), 3.59–3.71 (m, 2H, NCH_2), 3.94 (s, 6H, $2 \times OCH_3$), 5.99 (s, 2H, OCH_2O), 6.09 (s, 2H, OCH_2O), 6.53 (s, 2H, $2 \times Ar-H$), 7.19–7.44 (m, 5H, $5 \times Ar-H$); ^{13}C NMR ($CDCl_3$, 75 MHz, δ ppm): δ 54.9, 56.7, 59.7, 101.7, 109.2, 110.7, 127.2, 128.5, 129.3, 129.4, 134.8, 138.9, 142.8, 145.7; IR (KBr, cm^{-1}): ν 3448, 2861, 2359, 1639, 1432, 1384, 1301, 1141, 1096, 1051, 747, 712; ESI-MS: m/z 434 $[M + H]^+$; HRMS (ESI m/z) for $C_{25}H_{24}NO_6$ calcd 434.1604, found 434.1608 $[M + H]^+$.

5.4.5. 6-Propyl-3,9-dimethoxy-1,2-methylenedioxy-10,11-methylenedioxy-6,7-dihydro-5H-dibenz[c,e]azepine (**4e**)

The title compound was obtained starting from **3** and n-propylamine. As a white solid, yield: 79%; mp: 138–140 °C. Analytical data for **4e**: 1H NMR ($CDCl_3$, 300 MHz, δ ppm): 0.97 (t, 3H, CH_3 , $J = 7.2$ Hz), 1.57–1.65 (m, 2H, CH_2CH_2), 2.42–2.59 (m, 2H, NCH_2), 3.20 (d, 2H, NCH_2 , $J = 12.6$ Hz), 3.54 (d, 2H, NCH_2 , $J = 12.6$ Hz), 3.95 (s, 6H, $2 \times OCH_3$), 5.99 (s, 2H, OCH_2O), 6.09 (s, 2H, OCH_2O), 6.57 (s, 2H, $2 \times Ar-H$); ^{13}C NMR ($CDCl_3$, 75 MHz, δ ppm): δ 12.1, 21.0, 55.0, 56.8, 57.3, 101.7, 109.3, 110.6, 129.1, 134.9, 142.8, 145.7; IR (KBr, cm^{-1}): ν 3588, 3568, 3448, 2949, 2867, 1641, 1489, 1466, 1432, 1384, 1305, 1161, 1141, 1100, 1049, 753, 694; ESI-MS: m/z 386 $[M + H]^+$; HRMS (ESI m/z) for $C_{21}H_{24}NO_6$ calcd 386.1604, found 386.1609 $[M + H]^+$.

5.4.6. 6-Phenyl-3,9-dimethoxy-1,2-methylenedioxy-10,11-methylenedioxy-6,7-dihydro-5H-dibenz[c,e]azepine (**4f**)

The title compound was obtained starting from **3** and aniline. As a white solid, yield: 81%; mp: 231–232 °C. Analytical data for **4f**: 1H NMR ($CDCl_3$, 300 MHz, δ ppm): 3.83 (d, 2H, NCH_2 , $J = 12.9$ Hz), 3.88 (s, 6H, $2 \times OCH_3$), 4.32 (d, 2H, NCH_2 , $J = 12.9$ Hz), 6.00 (s, 2H, OCH_2O), 6.11 (s, 2H, OCH_2O), 6.54 (s, 2H, $2 \times Ar-H$), 6.81–7.30 (m, 5H, $5 \times Ar-H$); ^{13}C NMR ($CDCl_3$, 75 MHz, δ ppm): δ 52.0, 56.7, 59.7, 101.8, 109.0, 110.4, 115.2, 118.5, 129.2, 129.6, 134.8, 143.1, 145.7; IR (KBr, cm^{-1}): ν 3587, 3567, 3448, 2891, 1641, 1596, 1384, 1210, 1141, 1099, 1048, 753, 695; ESI-MS: m/z 420 $[M + H]^+$; HRMS (ESI m/z) for $C_{24}H_{22}NO_6$ calcd 420.1447, found 420.1452 $[M + H]^+$.

5.4.7. 6-Methyl-3,9-dimethoxy-1,2-methylenedioxy-10,11-methylenedioxy-6,7-dihydro-5H-dibenz[c,e]azepine (**4g**)

The title compound was obtained starting from **3** and methylamine hydrochloride. As a white solid, yield: 85%; mp: 180–182 °C. Analytical data for **4g**: 1H NMR ($CDCl_3$, 300 MHz, δ ppm): 2.45 (s, 3H, CH_3), 3.28 (d, 2H, NCH_2 , $J = 12.3$ Hz), 3.46 (d, 2H, NCH_2 , $J = 12.3$ Hz), 3.95 (s, 6H, $2 \times OCH_3$), 6.00 (s, 2H, OCH_2O), 6.10 (s, 2H, OCH_2O), 6.60 (s, 2H, $2 \times Ar-H$); ^{13}C NMR ($CDCl_3$, 75 MHz, δ ppm): δ 42.7, 56.7, 56.8, 101.8, 109.4, 110.4, 128.4, 135.1, 142.9, 145.8; IR (KBr, cm^{-1}): ν 3448, 2779, 1641, 1487, 1434, 1384, 1310, 1166, 1136, 1098, 1045, 706; ESI-MS: m/z 358 $[M + H]^+$; HRMS (ESI m/z) for $C_{19}H_{20}NO_6$ calcd 358.1291, found 358.1295 $[M + H]^+$.

5.4.8. 6-Phenethyl-3,9-dimethoxy-1,2-methylenedioxy-10,11-methylenedioxy-6,7-dihydro-5H-dibenz[*c,e*]azepine (**4h**)

The title compound was obtained starting from **3** and 2-phenethylamine. As a white solid, yield: 82%; mp: 138–140 °C. Analytical data for **4h**: ¹H NMR (CDCl₃, 300 MHz, δ ppm): 2.65–2.85 (m, 2H, NCH₂CH₂), 2.86–2.93 (m, 2H, NCH₂CH₂), 3.26 (d, 2H, NCH₂, *J* = 12.5 Hz), 3.60 (d, 2H, NCH₂, *J* = 12.5 Hz), 3.93 (s, 6H, 2 × OCH₃), 5.93 (s, 2H, OCH₂O), 5.99 (s, 2H, OCH₂O), 6.09 (s, 2H, OCH₂O), 6.55 (s, 2H, 2 × Ar–H), 7.19–7.33 (m, 5H, 5 × Ar–H); ¹³C NMR (CDCl₃, 75 MHz, δ ppm): δ 35.0, 55.2, 56.7, 57.4, 101.7, 109.2, 110.7, 126.2, 128.5, 128.7, 129.2, 134.9, 140.3, 142.9, 145.7; IR (KBr, cm⁻¹): ν 3567, 3448, 2808, 1639, 1487, 1434, 1384, 1304, 1136, 1107, 1048, 759, 700; ESI-MS: *m/z* 448 [M + H]⁺; HRMS (ESI *m/z*) for C₂₆H₂₆NO₆ calcd 448.1760, found 448.1765 [M + H]⁺.

5.4.9. 6-[2-(3,4-Methylenedioxy)phenyl]ethyl-3,9-dimethoxy-1,2-methylenedioxy-10,11-methylenedioxy-6,7-dihydro-5H-dibenz[*c,e*]azepine (**4i**)

The title compound was obtained starting from **3** and 3,4-methylenedioxyphenethylamine hydrochloride. As a white solid, yield: 81%; mp: 149–150 °C. Analytical data for **4i**: ¹H NMR (CDCl₃, 300 MHz, δ ppm): 2.60–2.70 (m, 2H, NCH₂CH₂), 2.73–2.86 (m, 2H, NCH₂CH₂), 3.24 (d, 2H, NCH₂, *J* = 12.5 Hz), 3.58 (d, 2H, NCH₂, *J* = 12.5 Hz), 3.94 (s, 6H, 2 × OCH₃), 5.93 (s, 2H, OCH₂O), 5.99 (s, 2H, OCH₂O), 6.09 (s, 2H, OCH₂O), 6.55 (s, 2H, 2 × Ar–H), 6.64–6.78 (m, 3H, 2 × Ar–H); ¹³C NMR (CDCl₃, 75 MHz, δ ppm): δ 34.7, 55.3, 56.8, 57.6, 100.9, 101.8, 108.3, 109.1, 109.2, 110.7, 121.5, 129.2, 134.1, 134.9, 142.9, 145.8, 145.9, 147.7; IR (KBr, cm⁻¹): ν 3447, 2914, 2802, 1640, 1502, 1489, 1431, 1384, 1303, 1138, 1099, 1048, 1024, 750, 662; ESI-MS: *m/z* 492 [M + H]⁺; HRMS (ESI *m/z*) for C₂₇H₂₆NO₈ calcd 492.1658, found 492.1665 [M + H]⁺.

5.4.10. 6-Hydroxyethyl-3,9-dimethoxy-1,2-methylenedioxy-10,11-methylenedioxy-6,7-dihydro-5H-dibenz[*c,e*]azepine (**4j**)

The title compound was obtained starting from **3** and ethanolamine. As a white solid, yield: 84%; mp: 100–101 °C. Analytical data for **4j**: ¹H NMR (CDCl₃, 300 MHz, δ ppm): 2.68–2.77 (m, 1H, NH₂), 2.95–3.03 (m, 1H, NH₂), 3.37 (d, 2H, NCH₂, *J* 12.6 Hz), 3.69 (d, 2H, NCH₂, *J* 12.6 Hz), 3.83 (t, 2H, OCH₂, *J* 5.1 Hz), 3.96 (s, 6H, 2 OCH₃), 6.01 (s, 2H, OCH₂O), 6.10 (s, 2H, OCH₂O), 6.63 (s, 2H, 2 Ar–H); ¹³C NMR (CDCl₃, 75 MHz, δ ppm): δ 54.9, 56.5, 56.8, 58.5, 101.7, 109.3, 110.6, 128.7, 135.0, 142.9, 145.8; IR (KBr, cm⁻¹): ν 3588, 3568, 3448, 1638, 1384, 1307, 1145, 1095, 1042, 635; ESI-MS: *m/z* 388 [M + H]⁺; HRMS (ESI *m/z*) for C₂₀H₂₂NO₇ calcd 388.1396, found 388.1402 [M + H]⁺.

5.5. General procedure for the preparation of **5a–d**

To the solution of **4a–d** (0.70 mmol) in CH₂Cl₂ (10 mL) were added hexadecyl trimethyl ammonium bromide (510 mg, 1.40 mmol) and KMnO₄ (222 mg, 1.40 mmol). After reflux for 0.5–1 h, the reaction mixture was cooled to room temperature, and then saturated aqueous NaHSO₃ solution was added with vigorous stirring. The reaction mixture was diluted with water, extracted with CH₂Cl₂ and the organic layer was washed with brine, dried with anhydrous sodium sulfate, filtered and evaporated in vacuum. The crude product was purified by column chromatography (CH₂Cl₂/EtOAc = 10:1–5:1) to yield **5a–d**, respectively, as a white solid.

5.5.1. 6-Ethyl-3,9-dimethoxy-1,2-methylenedioxy-10,11-methylenedioxy-6,7-dihydro-dibenz[*c,e*]azepine-5-one (**5a**)

The title compound was obtained starting from **4a**. As a white solid, yield: 43%; mp: 125–127 °C. Analytical data for **5a**: ¹H NMR (CDCl₃, 300 MHz, δ ppm): 1.21 (t, 3H, CH₃, *J* = 7.2 Hz), 3.29–3.41

(m, 1H, NCH₂), 3.72–3.87 (m, 1H, NCH₂), 3.83 (d, 1H, NCH₂, *J* = 14.6 Hz), 3.96 (s, 3H, OCH₃), 3.97 (s, 3H, OCH₃), 4.30 (d, 1H, NCH₂, *J* = 14.6 Hz), 5.95–6.13 (m, 4H, 2 × OCH₂O), 6.52 (s, 1H, Ar–H), 7.20 (s, 1H, Ar–H); ¹³C NMR (CDCl₃, 75 MHz, δ ppm): δ 13.5, 42.6, 50.9, 56.5, 57.0, 101.7, 102.0, 106.4, 108.7, 109.0, 109.7, 129.7, 133.1, 135.3, 136.7, 142.9, 143.2, 145.6, 147.2, 167.1; IR (KBr, cm⁻¹): ν 3587, 3567, 3448, 2985, 2920, 1637, 1419, 1384, 1316, 1166, 1140, 1098, 1045, 788, 756; ESI-MS: *m/z* 386 [M + H]⁺; HRMS (ESI *m/z*) for C₂₀H₂₀NO₇ calcd 386.1240, found 386.1244 [M + H]⁺.

5.5.2. 6-Butyl-3,9-dimethoxy-1,2-methylenedioxy-10,11-methylenedioxy-6,7-dihydro-dibenz[*c,e*]azepine-5-one (**5b**)

The title compound was obtained starting from **4b**. As a white solid, yield: 45%; mp: 162–163 °C. Analytical data for **5b**: ¹H NMR (CDCl₃, 300 MHz, δ ppm): 0.93 (t, 3H, CH₃, *J* = 7.2 Hz), 1.23–1.35 (m, 2H, CH₂), 1.53–1.65 (m, 2H, CH₂), 3.26–3.36 (m, 1H, NCH₂), 3.66–3.75 (m, 1H, NCH₂), 3.81 (d, 2H, NCH₂, *J* = 14.4 Hz), 3.95 (s, 3H, OCH₃), 3.97 (s, 3H, OCH₃), 4.30 (d, 2H, NCH₂, *J* = 14.4 Hz), 5.94–6.12 (m, 4H, 2 × OCH₂O), 6.52 (s, 1H, Ar–H), 7.23 (s, 1H, Ar–H); ¹³C NMR (CDCl₃, 75 MHz, δ ppm): δ 13.9, 20.1, 30.4, 47.6, 51.2, 56.5, 57.0, 101.7, 102.0, 106.5, 108.3, 108.9, 109.7, 129.8, 133.0, 135.3, 136.6, 143.2, 145.6, 147.1, 167.4; IR (KBr, cm⁻¹): ν 3567, 3448, 2955, 1641, 1618, 1602, 1426, 1384, 1310, 1166, 1139, 1099, 1045, 750, 697; ESI-MS: *m/z* 414 [M + H]⁺; HRMS (ESI *m/z*) for C₂₂H₂₄NO₇ calcd 414.1553, found 414.1558 [M + H]⁺.

5.5.3. 6-(Methoxycarbonyl)methyl-3,9-dimethoxy-1,2-methylenedioxy-10,11-methylenedioxy-6,7-dihydro-dibenz[*c,e*]azepine-5-one (**5c**)

The title compound was obtained starting from **4c**. As a white solid, yield: 40%; mp: 187–189 °C. Analytical data for **5c**: ¹H NMR (CDCl₃, 300 MHz, δ ppm): 3.75 (s, 3H, OCH₃), 3.78–3.89 (m, 2H, NCH₂), 3.95 (s, 3H, OCH₃), 3.97 (s, 3H, OCH₃), 4.52 (d, 1H, NCH₂, *J* = 15.0 Hz), 4.75 (d, 1H, NCH₂, *J* = 15.0 Hz), 5.95–6.14 (m, 4H, 2 × OCH₂O), 6.48 (s, H, Ar–H), 7.26 (s, H, Ar–H); ¹³C NMR (CDCl₃, 75 MHz, δ ppm): δ 48.7, 52.2, 52.3, 56.5, 57.0, 101.8, 102.1, 106.5, 108.5, 109.1, 110.1, 128.4, 132.0, 135.4, 137.1, 143.0, 143.2, 145.8, 168.0, 169.8; IR (KBr, cm⁻¹): ν 3588, 3568, 3448, 2366, 1634, 1608, 1422, 1384, 1163, 1140, 1098, 1051, 671; ESI-MS: *m/z* 430 [M + H]⁺; HRMS (ESI *m/z*) for C₂₁H₂₀NO₉ calcd 430.1138, found 430.1143 [M + H]⁺.

5.5.4. 6-Benzyl-3,9-dimethoxy-1,2-methylenedioxy-10,11-methylenedioxy-6,7-dihydro-dibenz[*c,e*]azepine-5-one (**5d**)

The title compound was obtained starting from **4d**. As a white solid, yield: 41%; mp: 170–171 °C. Analytical data for **5d**: ¹H NMR (CDCl₃, 300 MHz, δ ppm): 3.75–3.86 (m, 1H, PhCH₂), 3.81 (s, 3H, OCH₃), 3.99 (s, 3H, OCH₃), 4.26 (d, 1H, PhCH₂, *J* = 14.5 Hz), 4.59 (d, 1H, NCH₂, *J* = 14.8 Hz), 4.93 (d, 1H, NCH₂, *J* = 14.8 Hz), 5.96–6.10 (m, 4H, 2 × OCH₂O), 6.14 (s, 1H, Ar–H), 7.26 (s, 1H, Ar–H), 7.28–7.35 (m, 5H, 5 × Ar–H); ¹³C NMR (CDCl₃, 75 MHz, δ ppm): δ 50.3, 50.5, 56.6, 56.7, 101.7, 101.9, 106.4, 108.5, 109.1, 109.9, 127.5, 128.4, 128.6, 129.3, 132.4, 135.1, 137.3, 142.8, 143.2, 145.7, 147.0, 167.9; IR (KBr, cm⁻¹): ν 3450, 1637, 1611, 1431, 1384, 1310, 1169, 1142, 1104, 1054, 753, 694; ESI-MS: *m/z* 448 [M + H]⁺; HRMS (ESI *m/z*) for C₂₅H₂₂NO₇ calcd 448.1396, found 448.1402 [M + H]⁺.

5.6. Biological assays

5.6.1. Cytotoxicity assay

1 × 10⁴ K562 and K562/A02 cells were seeded in 96-well plates in RPMI-1640 and incubated for 24 h. The exponentially growing cancer cells were incubated with various concentrations of compounds for 72 h at 37 °C (5% CO₂, 95% humidity). After 72 h of incubation, MTS was added directly to the cells. After additional incubation for 3 h at 37 °C, the absorbance at 490 nm was read on

a microplate reader (Thermo, USA). The IC₅₀ values of the compounds for cytotoxicity were calculated by GraphPad Prism 3.0 software from the dose-response curves.

5.6.2. Flow cytometric analysis

1 × 10⁶ K562/A02 or K562 cells in culture were pre-incubated with different concentrations of the target compounds, VRP or vehicle control (0.1% DMSO) for 1 h at 37 °C, followed by addition of 0.5 μM Rh123 or ADR and incubation for 30 min, respectively. The reaction was stopped by addition of ice-cold PBS and centrifugation, washed with ice-cold PBS three times, and subjected analysis by flow cytometry. The relative values were identified by dividing the fluorescence intensity of each measurement by that of vehicle control.

5.6.3. Western blot analysis

K562/A02 cells were incubated with 5 μM individual compound or vehicle control for 48 h, respectively. Following incubation, the cells were harvested and lysed. The cell lysates (30 μg) were separated by SDS-PAGE (12% gel) and transferred onto a PVDF membrane. After blocked in a solution containing 5% non-fat milk in TBST buffer, the target proteins were probed with anti-P-gp, anti-GAPDH, respectively. Subsequently, the membranes were washed with TBST buffer and incubated with horseradish peroxidase-conjugated secondary antibody. After additional washes with TBST buffer, the protein-antibody complex were visualized by the enhanced Phototope TM-HRP Detection Kit (Cell Signaling, USA) and exposed to Kodak medical X-ray processor (Kodak, USA).

5.6.4. RT-PCR analysis

K562/A02 cells were seeded in 6-well plates at a density of 5 × 10⁵ cells and then cultured without or with target compounds (5 μM) for 48 h. Total RNA was extracted and then reverse transcribed from mRNA to cDNA using the RT-PCR kit (Promega, WI, USA). The PCR profile was as follows: 10 min at 95 °C, followed by 30 cycles of 30 s at 95 °C and 1 min at 60 °C. The standard curve and data analysis were produced using Bio-Rad iQ5 software. The relative mRNA level treated with inhibitors was expressed as fold change of the control (in the presence of 0.1% DMSO).

5.6.5. Duration of the MDR-reversal activity of **4i**

1 × 10⁵ cells were plated in 96-well plates and cultured overnight, followed by incubation with **4i** (2.5 μM) or VRP (10 μM) for 24 h. Then, the cells were washed with PBS three times and resuspended in complete medium. Various concentrations of ADR was added to the culture at predefined intervals (0, 6, 12, and 24 h) after removal of **4i** or VRP, and incubated for an additional 72 h (5% CO₂, 95% humidity). MTS was added and absorbance at 490 nm was read on a microplate reader (Thermo, USA). The IC₅₀ values of the compounds for cytotoxicity were calculated by GraphPad Prism 3.0 software from the dose-response curves.

5.6.6. P-gp ATPase assay

Drug-stimulated activity of P-gp ATPase was detected by P-gp-Glo™ assay system (Promega, USA). By following the user protocol provided by the vender, the activity of P-gp ATPase was measured in the presence or absence of 200 μM Na₃VO₄, 200 μM VRP (as a positive reference), 40 μM **4i**. The luminescence of the sample reflects the ATP level in the sample, which is negatively correlated with the activity of P-gp ATPase and was detected in a luminometer (Perkin Elmer TD-20, USA).

Acknowledgements

The work was financially supported by the Innovative Program for Postgraduate Students of Jiangsu province (NO. CX10B-372Z)

and National Natural Science Foundation of China grant No. 30873083 and 81173082, respectively. We thank to Prof. Dongsheng Xiong (Institute of Hematology & Blood Diseases Hospital, CAMS & PUMC, China) for providing K562 and K562/A02 cell lines.

Appendix A. Supplementary material

Supplementary material associated with this article can be found, in the online version, at doi:10.1016/j.ejmech.2012.02.034.

References

- [1] P.D. Eckford, F.J. Sharom, ABC efflux pump-based resistance to chemotherapy drugs, *Chem. Rev.* 109 (2009) 2989–3011.
- [2] D. Turk, M.D. Hall, B.F. Chu, J.A. Ludwig, H.M. Fales, M.M. Gottesman, G. Szakacs, Identification of compounds selectively killing multidrug-resistant cancer cells, *Cancer Res.* 69 (2009) 8293–8301.
- [3] C. Martelli, D. Alderighi, M. Coronello, S. Dei, M. Frosini, B. Le Bozec, D. Manetti, A. Neri, M.N. Romanelli, M. Salerno, S. Scapecchi, E. Mini, G. Sgaragli, E. Teodori, N,N-bis(cyclohexanol)amine aryl esters: a new class of highly potent transporter-dependent multidrug resistance inhibitors, *J. Med. Chem.* 52 (2009) 807–817.
- [4] L. Zhang, S. Ma, Efflux pump inhibitors: a strategy to combat P-glycoprotein and the NorA multidrug resistance pump, *ChemMedChem* 5 (2010) 811–822.
- [5] E. Crowley, C.A. McDevitt, R. Callaghan, Generating inhibitors of P-glycoprotein: where to, now? *Methods Mol. Biol.* 596 (2010) 405–432.
- [6] C.P. Wu, A.M. Calcagno, S.V. Ambudkar, Reversal of ABC drug transporter-mediated multidrug resistance in cancer cells: evaluation of current strategies, *Curr. Mol. Pharmacol.* 1 (2008) 93–105.
- [7] C.P. Wu, S. Ohnuma, S.V. Ambudkar, Discovering natural product modulators to overcome multidrug resistance in cancer chemotherapy, *Curr. Pharm. Biotechnol.* 12 (2011) 609–620.
- [8] H.H. Yoo, M. Lee, M.W. Lee, S.Y. Lim, J. Shin, D.H. Kim, Effects of Schisandra lignans on P-glycoprotein-mediated drug efflux in human intestinal Caco-2, *Planta Med.* 73 (2007) 444–450.
- [9] W.F. Fong, C.K. Wan, G.Y. Zhu, A. Chattopadhyay, S. Dey, Z. Zhao, X.L. Shen, Schisandrol A from Schisandra chinensis reverses P-glycoprotein-mediated multidrug resistance by affecting Pgp-substrate complexes, *Planta Med.* 73 (2007) 212–220.
- [10] J.B. Chang, Q. Wang, Y.F. Li, Synthesis and biological activity of Wuweizisu C and analogs, *Curr. Top. Med. Chem.* 9 (2009) 1660–1675.
- [11] J. Jin, H. Sun, H. Wei, G. Liu, The anti-hepatitis drug DDB chemosensitizes multidrug resistant cancer cells in vitro and in vivo by inhibiting P-gp and enhancing apoptosis, *Invest. New Drugs* 25 (2007) 95–105.
- [12] F. Klepsch, T. Stockner, T. Erker, M. Muller, P. Chiba, G.F. Ecker, Using structural and mechanistic information to design novel inhibitors/substrates of P-glycoprotein, *Curr. Top. Med. Chem.* 10 (2010) 1769–1774.
- [13] C. Martelli, M. Coronello, S. Dei, D. Manetti, F. Orlandi, S. Scapecchi, M. Novella Romanelli, M. Salerno, E. Mini, E. Teodori, Structure-activity relationships studies in a series of N,N-bis(alkanol)amine aryl esters as P-glycoprotein (Pgp) dependent multidrug resistance (MDR) inhibitors, *J. Med. Chem.* 53 (2010) 1755–1762.
- [14] T.J. Raub, P-glycoprotein recognition of substrates and circumvention through rational drug design, *Mol. Pharm.* 3 (2006) 3–25.
- [15] N.A. Colabufo, F. Berardi, M. Cantore, M. Contino, C. Inglese, M. Niso, R. Perrone, Perspectives of P-glycoprotein modulating agents in oncology and neurodegenerative diseases, *J. Med. Chem.* 53 (2010) 1883–1897.
- [16] C. Baumert, A. Hilgeroth, Recent advances in the development of P-gp inhibitors, *Anticancer Agents Med. Chem.* 9 (2009) 415–436.
- [17] J. Chang, R. Chen, R. Guo, C. Dong, K. Zhao, Synthesis, separation, and theoretical studies Of chiral biphenyl lignans (α- and β-DDB), *Helv. Chim. Acta* 86 (2003) 2239–2246.
- [18] C.L. Dai, A.K. Tiwari, C.P. Wu, X.D. Su, S.R. Wang, D.G. Liu, C.R. Ashby Jr., Y. Huang, R.W. Robey, Y.J. Liang, L.M. Chen, C.J. Shi, S.V. Ambudkar, Z.S. Chen, L.W. Fu, Lapatinib (Tykerb, GW572016) reverses multidrug resistance in cancer cells by inhibiting the activity of ATP-binding cassette subfamily B member 1 and G member 2, *Cancer Res.* 68 (2008) 7905–7914.
- [19] S. Krawczyk, M. Otto, A. Otto, C. Coburger, M. Krug, M. Seifert, V. Tell, J. Molnar, A. Hilgeroth, Discovery of pyridine-2-ones as novel class of multidrug resistance (MDR) modulators: first structure-activity relationships, *Bioorg. Med. Chem.* 19 (2011) 6309–6315.
- [20] Y.M. Wang, L.X. Hu, Z.M. Liu, X.F. You, S.H. Zhang, J.R. Qu, Z.R. Li, Y. Li, W.J. Kong, H.W. He, R.G. Shao, L.R. Zhang, Z.G. Peng, D.W. Boykin, J.D. Jiang, N-(2,6-dimethoxypyridine-3-yl)-9-methylcarbazole-3-sulfonamide as a novel tubulin ligand against human cancer, *Clin. Cancer Res.* 14 (2008) 6218–6227.
- [21] W.L. Wu, S.E. Chen, W.L. Chang, C.F. Chen, A.R. Lee, Synthesis and anti-hepatotoxicity of some Wuweizisu analogues, *Eur. J. Med. Chem.* 27 (1992) 353–358.